

## Modeling of Ice-Water Phase Change in Horizontal Annulus Using Modified Enthalpy Method

Esad Tombarević\* and Igor Vušanović

*Faculty of Mechanical Engineering, University of Montenegro, Cetinjski put bb, 81000 Podgorica, Montenegro*

Received 30 December 2009; Accepted (in revised version) 29 September 2010

Available online 28 February 2011

---

**Abstract.** Phase change in ice-water systems in the geometry of horizontal cylindrical annulus with constant inner wall temperature and adiabatic outer wall is modeled with an enthalpy-based mixture model. Solidification and melting phenomena under different temperature conditions are analyzed through a sequence of numerical calculations. In the case of freezing of water, the importance of convection and conduction as well as the influence of cold pipe temperature on time for the complete solidification are examined. As for the case of melting of ice, the influence of the inner pipe wall temperature on the shape of the ice-water interface, the flow and temperature fields in the liquid, the heat transfer coefficients and the rate of melting are analyzed. The results of numerical calculations point to good qualitative agreement with the available experimental and other numerical results.

**AMS subject classifications:** 80A22

**Key words:** Phase change, solidification, melting, enthalpy model, fixed grid, annulus.

---

### 1 Introduction

Modeling of solid-liquid phase change phenomena has received a lot of attention since it is a common occurrence in metallurgical processes, latent heat thermal energy storages, oceanography, food processing, nuclear reactor safety etc. The nature of solid-liquid phase change can take different forms [1–3]. In the case of water and pure substances, the phase-change transition occurs at a constant temperature and a smooth continuous front separates the solid and the liquid phase distinctively, whereby different physical properties characterize the phases. The solidification of metal alloys and other multicomponent systems occurs at a finite temperature interval, and therefore a phase-change region (the "mushy" zone) forms, containing the solid and the liquid phase at the equilibrium temperature. The solid phase in the two-phase region

---

\*Corresponding author.

Email: esadt@ac.me (E. Tombarević), igorvus@ac.me (I. Vušanović)

can be formed as a rigid dendrite structure with a complex shape, or in the form of free floating particles which can be advected with the flow through or out of the mushy region. During the solidification of waxes, polymers and glasses, the liquid and the solid phase are dispersed throughout the phase-change region without creating a distinct solid-liquid interface.

The position of the solid-liquid front which propagates as the phase change proceeds, cannot be determined in advance, and it has to be determined as an unknown variable, together with the temperature field in both phases and the fluid flow in the liquid phase and the mushy region. The temperature fields in the solid and the liquid phase can be obtained from the energy conservation equations for solid and liquid phase respectively, while the fluid flow in the liquid is usually calculated from the momentum and the mass balance equation in the liquid. The transition of the solid-liquid interface is determined based on the interface energy balance equation which includes latent heat ( $L$ ) as the key parameter in the phase-change process. The fluid flow is usually driven by buoyancy forces caused by the thermal gradients in the liquid phase. Several alternative numerical methods have been proposed for the solution of heat transfer with phase change that is usually referred to as the Stefan problem [4]. A survey of various numerical techniques can be found in Crank [5] and Voller [6]. One of the key challenges that have been the focus of research in the past is tracking the transient phase change interface which is usually treated with moving or fixed grid methods.

The moving grid methods (or variable grid, deforming grid, front tracking methods) [7,8] assume the fixing of the solid-liquid interface in each time step and solving the conservation equations separately for the solid and the liquid phase. The interface position has to be calculated for each time step using the classical Stefan formulation. As the solid-liquid interface propagates with time, the separate numerical grids for the solid and the liquid phase need to be rearranged (deformed) in each time step, to ensure that the node points are always on the phase-change front, which requires special techniques for meshing the domain.

The fixed grid methods (or enthalpy methods) [9,10] for phase change problems are based on one set of equations for both phases. A review of fixed grid techniques for phase-change problems can be found in Voller [9]. The phase change is taken into account with the appropriate source terms in the momentum and energy equations. The fluid flow in the two-phase region is usually described by Darcy law [10]. The phase-change material is treated as a mixture, with unique physical properties depending only on liquid fraction ( $g_s$ ) as a parameter. The main advantage of these methods is that there is no need to explicitly track the solid-liquid interface.

In this paper, an enthalpy-based model is applied to simulate the solid-liquid phase change in water, for the geometry of cylindrical horizontal annulus. This kind of geometry is widely used for thermal energy storage applications. Thermal energy storage based on solid-liquid phase change is a well-known and widely used solution used in air conditioning facilities, known to be a cost-effective measure. A valuable reference resource on thermal energy storage systems and applications is a book by

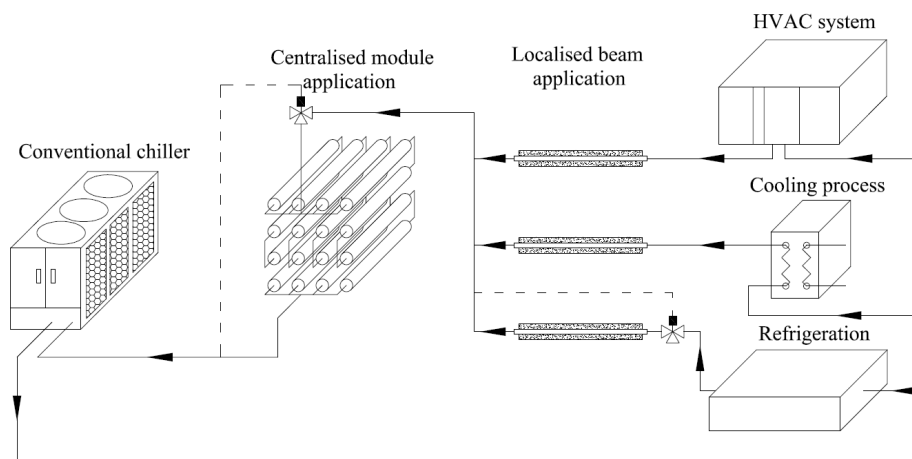


Figure 1: Ice storage and its integration in the system with chiller and consumers.

Dinçer and Rosen [11]. Zalba et al. [12] provide a historical overview of thermal energy storages with solid-liquid phase change, with emphasis on used phase-change materials, heat transfer and applications. A recent review of research on cold thermal energy storage is given in a paper by Saito [13].

Low temperature energy is usually stored in solid form during the night, when the freezing of phase-change material (water) occurs. Afterwards, in the daytime regime, the accumulated low temperature energy is released by the melting of the same phase-change material, and then used to cover the cooling load partially or completely.

One typical configuration of ice storage consists of a module with horizontal beams in which primary fluid flows through the inner beam pipe and the phase-change material (water or eutectic salts) in the annular space freezes in the charging and melts in the discharging operation mode. This configuration of ice storage and its integration in the system with a chiller and consumers is sketched in Fig. 1.

Appropriate dimensioning and the design of ice storage equipment requires profound understanding of the phase-change phenomenon that occurs in the charging and the discharging operation mode. The configuration of the horizontal annulus is studied theoretically and experimentally and a comprehensive review is given in Yao and Prusa [14]. Experimental results for this particular geometry can be found in a paper by White et al. [15], while numerical results obtained by applying fixed grid temperature based method are presented in Ho and Chen [16].

## 2 Physical and mathematical model

The physical model considered in this work is a unit length horizontal circular annulus with the inner pipe radius  $r_i$  and the outer pipe radius  $r_o$  (Fig. 2). The temperature of the inner pipe  $T_w$  is assumed to be constant and uniform along the pipe. In the case of freezing, the water in the annular space is initially at temperature  $T_i$  and the freezing

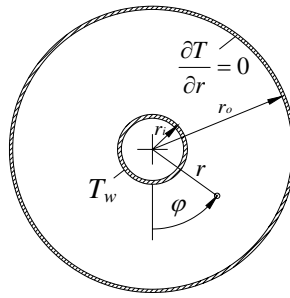


Figure 2: Physical model.

starts when the inner pipe temperature is suddenly reduced below the phase change temperature. As for melting, the ice in the annular space is initially at temperature  $T_i$  and the melting starts when the inner pipe temperature is suddenly increased above the phase-change temperature.

Due to its simplicity, the fixed grid enthalpy-based method is applied for modeling phase change in this study. The mixture conservation equations for mass, momentum and energy, together with property equations of ice and water, represent a closed system which solution is a time dependant flow and the temperature fields in the annulus. The flow field is considered to be two dimensional, laminar and incompressible. The physical properties of water and ice shown in Table 1 are temperature invariant, except for the water density, whose nonlinear variation with temperature (Fig. 3) is included in the buoyancy term in the momentum equation.

Nonlinear variation of water density with temperature can be represented using the fourth order polynomial:

$$\rho = 999.840281167 + 0.0673268037314T - 0.00894484552601T^2 + 8.78462866500 \times 10^{-5}T^3 - 6.62139792627 \times 10^{-7}T^4. \tag{2.1}$$

The thermal expansion coefficient is obtained by differentiating the above given formula, and in the same temperature range is given in Fig. 4. It can be also given as a fourth order polynomial:

$$\beta = (-0.66443347028 + 0.17869952437T - 0.00264710551T^2 + 0.00002794300T^3 - 0.00000001805443T^4) \times 10^{-4}. \tag{2.2}$$

For the derivation of mixture conservation equations of mass, momentum and energy, the averaging technique originally proposed by Bennon and Incropera [17] is

Table 1: The physical properties of ice and water.

Physical parameter		Water	Ice
$\rho$ on 0 °C	[kg/m <sup>3</sup> ]	999.84	916.7
$c_p$	[J/kgK]	4202.0	2040.0
$\lambda$	[W/mK]	0.56	2.26
$\mu$	[Pas]	0.001547	-

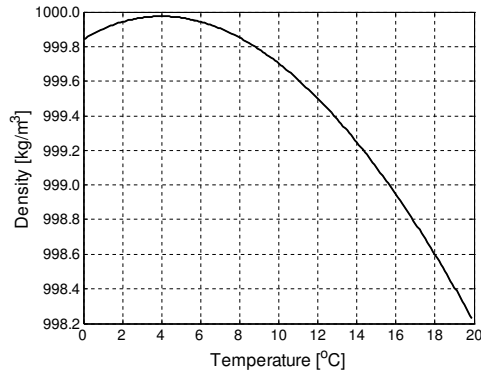


Figure 3: The density of water as a function of temperature.

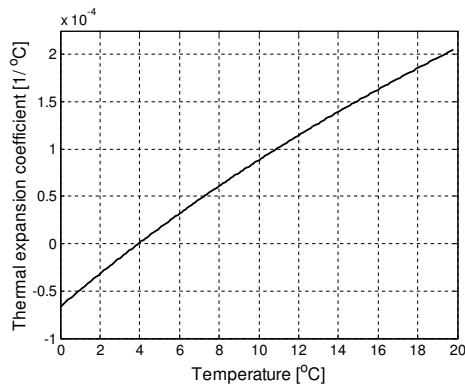


Figure 4: Thermal expansion coefficient as a function of temperature.

applied for ice-water system. Equations are written for each phase separately, and then summed in order to obtain equations of a single model. Based on the enthalpy method, the governing equations in polar coordinates, given in a form suitable for numerical integration with control volume method [18], are as follows:

Continuity equation

$$\frac{\partial \rho}{\partial t} + \nabla \cdot (\rho \vec{V}) = 0. \tag{2.3}$$

Momentum equations

$$\begin{aligned} & \frac{\partial}{\partial t}(\rho v_r) + \nabla \cdot (\rho \vec{V} v_r) - \frac{\rho v_\varphi^2}{r} \\ &= -\frac{\partial p}{\partial r} + \nabla \cdot (\mu \nabla v_r) - \mu \frac{v_r}{r^2} - \frac{2\mu}{r^2} \frac{\partial v_\varphi}{\partial \varphi} - \rho g \beta (T - T_{ref}) \sin \varphi + S_r, \end{aligned} \tag{2.4a}$$

$$\begin{aligned} & \frac{\partial}{\partial t}(\rho v_\varphi) + \nabla \cdot (\rho \vec{V} v_\varphi) + \frac{\rho v_r v_\varphi}{r} \\ &= -\frac{1}{r} \frac{\partial p}{\partial \varphi} + \nabla \cdot (\mu \nabla v_\varphi) - \mu \frac{v_\varphi}{r^2} + \frac{2\mu}{r^2} \frac{\partial v_r}{\partial \varphi} + \rho g \beta (T - T_{ref}) \cos \varphi + S_\varphi. \end{aligned} \tag{2.4b}$$

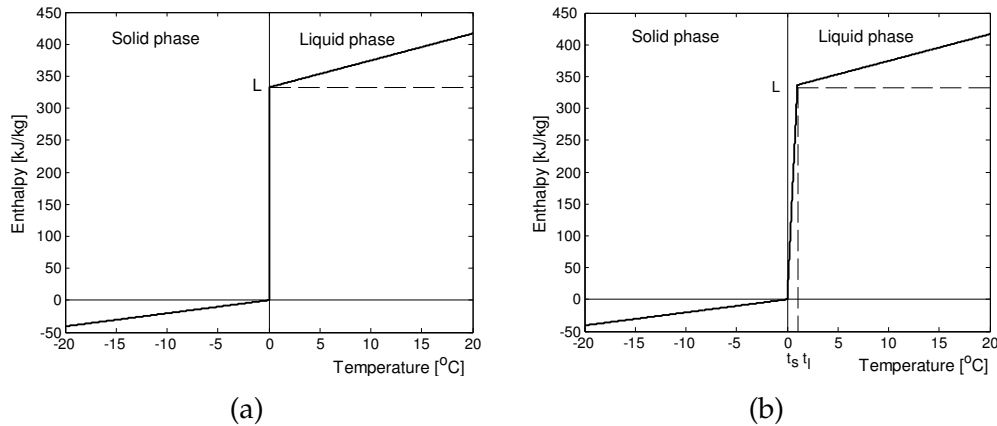


Figure 5: The enthalpy of water as a function of temperature.

Energy equation

$$\frac{\partial}{\partial t}(\rho h) + \nabla \cdot (\rho \vec{V} h) = \nabla \cdot (\lambda \nabla T) + S_h. \tag{2.5}$$

Enthalpy and temperature transition through the phase change is controlled with the source term  $S_h$  on the right hand side of the Eq. (2.5) which is obtained by dividing the total enthalpy  $H$  into its sensible  $h$  and the latent part  $\Delta H$ ,  $H = h + \Delta H$ :

$$S_h = - \left[ \frac{\partial}{\partial t}(\rho \Delta H) + \nabla \cdot (\rho \vec{V} L) \right]. \tag{2.6}$$

In reality, the phase change of water is isothermal and total enthalpy is a step function of temperature and has a jump on 0°C. This jump is equal to the value of the latent heat  $L$  (332.4 kJ/kg). In order to overcome this numerical problem, the jump of total enthalpy  $H$  at the constant phase-change temperature (Fig. 5(a)) is converted into a linear function  $\Delta H$  at the narrow temperature interval (Fig. 5(b)) so that that it mimics the isothermal nature of the phase change.

The latent heat  $\Delta H$  is expressed as a function of the volumetric fraction of liquid (porosity)  $g_l$  in the given control volume:

$$\Delta H = f(T) = \begin{cases} L, & T \geq T_l, \\ g_l \cdot L, & T_s \leq T < T_l, \\ 0, & T < T_s, \end{cases} \tag{2.7}$$

$T_l$  is the temperature at which the freezing process starts and  $T_s$  is the temperature at which it ends. In this work  $T_l = 0.01^\circ\text{C}$  and  $T_s = 0^\circ\text{C}$ . On the other hand, porosity can be given as a simple linear function of temperature:

$$g_l = \begin{cases} 1, & T \geq T_l, \\ \frac{T - T_s}{T_l - T_s}, & T_s \leq T < T_l, \\ 0, & T < T_s. \end{cases} \tag{2.8}$$

With this definition of porosity, physical properties in the mushy region ( $T_s < T < T_l$ ) can be expressed as:

$$\rho = (1 - g_l)\rho_s + g_l\rho_l, \quad (2.9a)$$

$$\lambda = (1 - g_l)\lambda_s + g_l\lambda_l. \quad (2.9b)$$

The energy equation (2.5) requires a special treatment because of the source term on the right hand side, which includes the latent enthalpy content  $\Delta H$ . To obtain the new enthalpy value  $h^{k+1}$  for the iteration step ( $k + 1$ ), one needs  $\Delta H^{k+1}$  which itself depends on the unknown solution  $h^{k+1}$ . The procedure for handling this problem and the details of numerical integration of energy equation are presented in the appendix of [10]. The final iterative scheme for the calculation of latent heat content  $\Delta H$  for the given control volume in the iteration step  $k + 1$  is:

$$\Delta H^{k+1} = \Delta H^k + h^k - c_p f^{-1}(\Delta H^k), \quad (2.10)$$

where  $f^{-1}$  is the inverse of the latent heat function given in (2.7).

During the calculation of the velocity field, the velocity at the control volume located in the solid phase should be nullified, while the velocities in the liquid phase should remain unaffected. Therefore, Darcy-like source terms  $S_r$  and  $S_\varphi$  are used in momentum equations (2.4a) and (2.4b) to provide the above mentioned conditions:

$$S_r = -C \frac{(1 - g_l)^2}{g_l^3 + q} v_r, \quad (2.11a)$$

$$S_\varphi = -C \frac{(1 - g_l)^2}{g_l^3 + q} v_\varphi. \quad (2.11b)$$

In the liquid phase  $g_l = 1$  and therefore source terms (2.11a) and (2.11b) are equal to zero, and momentum equations (2.4a) and (2.4b) have the standard form as for incompressible fluids. As liquid turns to solid (porosity  $g_l$  approaches zero), source terms become large enough so as to dominate in momentum equations, and suppress velocities in the solid phase. In this work  $C$  is set at 1600000. The constant  $q$  which is introduced to avoid division by zero as liquid turns to solid is set at 0.001.

Equations of mathematical model are discretized by control volume method [18]. A fully implicit scheme is used in time integration, and an upwind scheme for the approximation of convective fluxes on the control volume faces. The obtained algebraic equations are solved by iterative Gauss-Siedel algorithm. The SIMPLER algorithm and the staggered grid approach are used for pressure velocity coupling. Because of the symmetry of the temperature and flow fields (vertical centerline is the axis of symmetry), only one half of the domain is considered.

### 3 Results and discussions

A number of numerical calculations with different inner pipe wall temperatures are performed for the annulus with  $r_i = 12.7\text{mm}$  and  $r_o = 50.8\text{mm}$  in order to analyse the

phenomenon of freezing of water and melting of ice in this geometry. In both cases, the primary goal was to estimate the relative importance of convection and conduction on the process. In order to obtain results that are grid independent, calculations were carried out on grids of different densities ( $25 \times 50$ ,  $50 \times 100$  and  $100 \times 200$ ). Grid sensitivity trials resulted in a final grid of 5000 CV ( $50 \times 100$ ). Also, calculations were performed with different time step (1s, 5s and 10s), and the time step sensitivity analysis resulted in an optimum time step size of 5s.

### 3.1 Solidification

The temperature and the flow fields for the freezing of water at the initial temperature  $T_i = 10^\circ\text{C}$  and inner wall temperature  $T_w = -15^\circ\text{C}$  are shown in Fig. 6.

Due to the temperature gradients, natural convection is induced in the liquid phase. At the very beginning of the freezing process, only a counterclockwise cell appears in the liquid. The clockwise cell appears in the upper part of the annulus where the water maintains the highest temperature and thus the lowest density. As the freezing proceeds and the remaining liquid is cooled, the inversion of the flow field (counterclockwise to clockwise) occurs due to the water density anomaly. In the lower part of the annulus, next to the ice-water interface, another clockwise cell appears. On its outer side is the old cell and the line between those two cells lies on the  $4^\circ\text{C}$  isotherm. The inner cell expands with time and occupies most of the liquid region. After 1900 seconds, a small counterclockwise cell is observed at the bottom of the annulus. After 4500s only one clockwise cell exists, since the temperature in the liquid phase is below  $4^\circ\text{C}$ , the temperature at which the density maximum occurs. Ice is formed on the

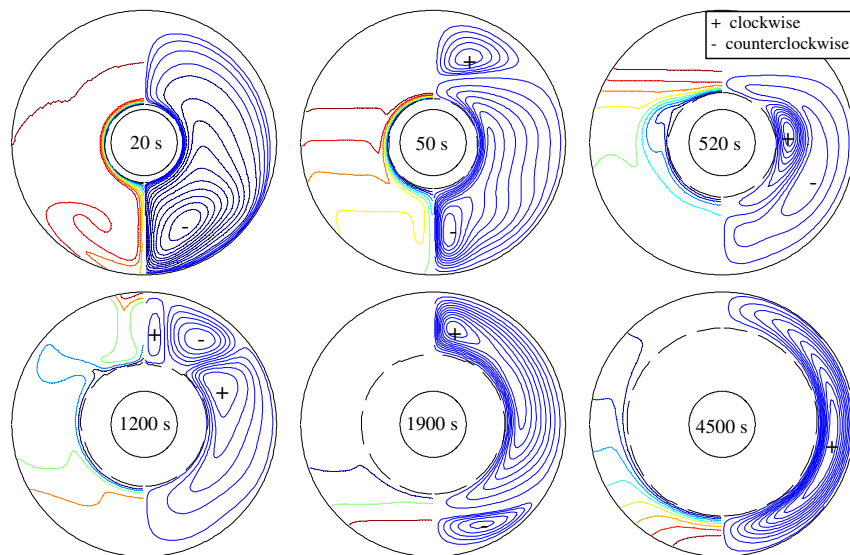


Figure 6: The temperature field (left) and the flow field (right) during the solidification at  $T_w = -15^\circ\text{C}$  and  $T_i = 10^\circ\text{C}$ .

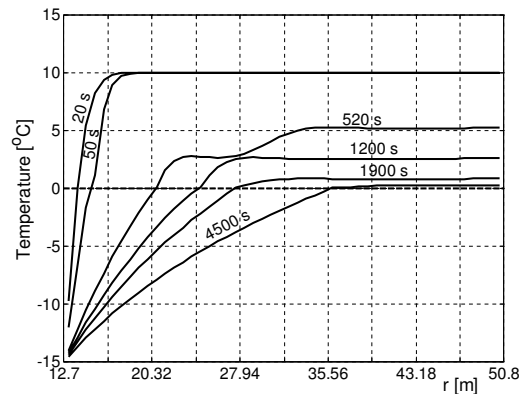


Figure 7: Temperature distribution along radial direction at  $\varphi = 90^\circ$ .

cold inner pipe and the water circulates in the annular space between the ice-water interface (dashed line) which is at a constant temperature of the phase change and the outer adiabatic wall. Therefore, with no flux boundary condition at the outer wall, the temperature of the remaining liquid decreases relatively fast towards the freezing point and the natural convection is retarded with time. To clarify this statement, the temperature distribution along radial direction at  $\varphi = 90^\circ$  in several time instants are plotted in Fig. 7. One can clearly note that the temperature of the bulk of the liquid decreases with time. With different boundary condition, such as constant temperature on the outer pipe wall, the temperature gradients in the liquid phase would be always present and may induce the fluid motion strong enough to have a noticeable effect on the shape of the surface of ice. This case was numerically investigated by using the moving grid method and the results are reported by Saitoh and Hirose [19].

The time for the complete solidification of water in the annulus is 12,190 seconds. Using the same model and neglecting the convection in the liquid phase (velocities are set to zero and only the energy equation is solved), the time needed for the complete solidification is 12,172 seconds. Therefore, because of much shorter computation time, the convection in the liquid phase is neglected in the further analysis of freezing cases.

The radial temperature profiles in the domain for several time instants for  $T_w = -15^\circ\text{C}$  and  $T_i = 10^\circ\text{C}$  are shown in Fig. 8. The temperature gradient in the solid phase  $\partial T_s / \partial r$  decreases with time as the thickness of the ice layer increases. On the other hand, the temperature of water falls to the phase-change temperature and after some time, the temperature gradient in the liquid phase  $\partial T_l / \partial r$  is almost equal to zero. At the same time, the rate of ice formation  $\partial r_s / \partial t$  (Fig. 9) decreases and the energy balance on ice water interface (3.1) is always satisfied:

$$\lambda_s \frac{\partial T_s}{\partial r} - \lambda_l \frac{\partial T_l}{\partial r} = \rho_s L \frac{\partial r_s}{\partial t}. \quad (3.1)$$

After 12,171 seconds, all the water in the annulus is frozen and the ice is quickly cooled down. The change of the thickness of ice layer with time for  $T_w = -5^\circ\text{C}$ ,  $-10^\circ\text{C}$  and

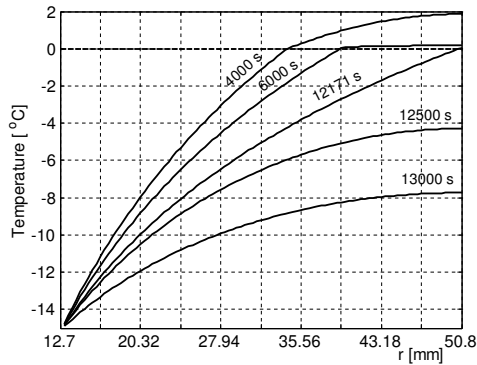


Figure 8: Temperature field in solid and liquid phase at several time instants for  $T_w = -15^\circ\text{C}$  and  $T_i = 10^\circ\text{C}$ .

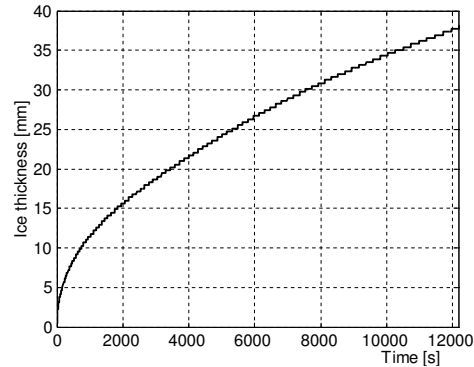


Figure 9: Change of the thickness of ice layer with time for  $T_w = -15^\circ\text{C}$  and  $T_i = 10^\circ\text{C}$ .

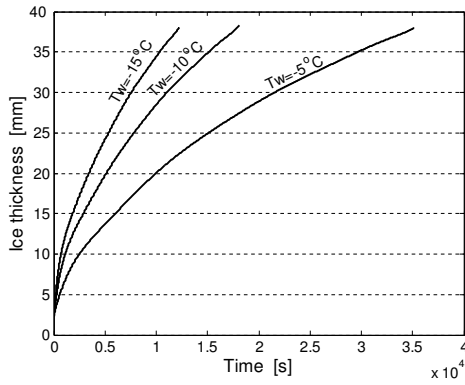


Figure 10: Change of the thickness of ice layer with time for  $T_w = -5^\circ\text{C}$ ,  $-10^\circ\text{C}$ ,  $-15^\circ\text{C}$  and  $T_i = 10^\circ\text{C}$ .

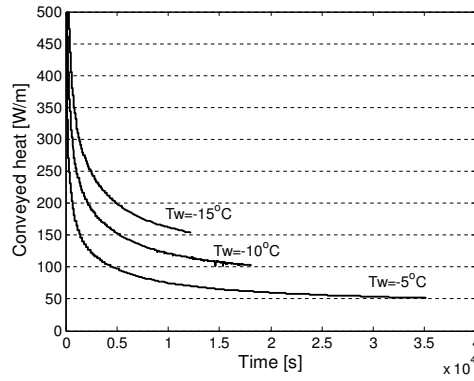


Figure 11: Heat conveyed over time for  $T_w = -5^\circ\text{C}$ ,  $-10^\circ\text{C}$ ,  $-15^\circ\text{C}$  and  $T_i = 10^\circ\text{C}$ .

$-15^\circ\text{C}$  is given in Fig. 10. The heat conveyed over the unit length of the inner pipe wall to the primary fluid in each time step could be approximately calculated as:

$$\dot{Q}(t) = (T_f - T_w) \left( \frac{1}{2\pi\lambda_s} \ln \frac{r_s(t)}{r_i} \right)^{-1}, \quad (3.2)$$

and is given in Fig. 11.

The conveyed heat decreases with time as the thickness of ice layer and the resistance to heat conduction increases. The area below those lines represents low temperature heat stored in the annulus. The time needed for the complete solidification of the water in the annulus strongly depends on the temperature  $T_w$ , as presented in Fig. 12 for the temperature range  $-40^\circ\text{C} - 0^\circ\text{C}$ .

### 3.2 Melting

The initial temperature of ice in all numerical simulations of melting is the phase change temperature  $0^\circ\text{C}$ . The temperature and the flow fields in several time instances

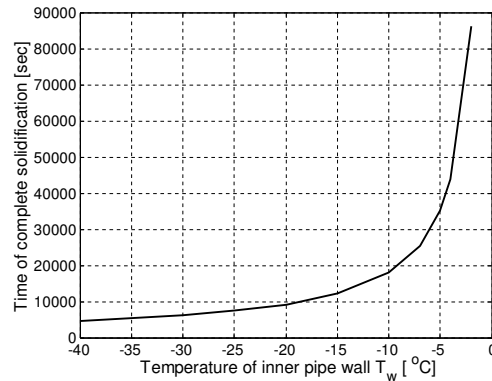


Figure 12: The time needed for the complete solidification as a function of  $T_w$ .

in the case of melting at  $T_w = 4^\circ\text{C}$  are illustrated in Fig. 13. At the beginning of melting, conduction is the dominant heat transfer mechanism and the solid-liquid phase change interface has the shape of a circle with the center on the axis of annulus. As melting continues, the convection in the liquid phase intensifies and causes the deformation of isotherms. In this case, the water in the vicinity of the inner pipe has the highest density and therefore flows downwards along the inner pipe, while the water in the vicinity of ice surface flows upwards.

Local heat transfer coefficients referring to the heat transfer from the pipe surface to the water as a function of the angle  $\varphi$  ( $\varphi = 0^\circ$  at the bottom and  $\varphi = 180^\circ$  at the top of annulus) are presented in Fig. 14. It is evident that the heat transfer is more intense on the top of the heat source since relatively cold water, previously cooled down during the flow along the ice surface, comes into contact with a source of heat. On the surface of ice, the opposite situation occurs—relatively warmer water comes in contact with the ice surface below the heat source and the consequence is a pear-shaped melted region facing downwards.  $\varphi$

In all cases at  $T_w > 4^\circ\text{C}$ , the isotherm  $T = 4^\circ\text{C}$ , i.e., the water featuring maximum density is located somewhere between the surface of the inner pipe and the surface of ice, and two distinct types of flow cells appear in the melted region. The temperature and the flow fields at several time points for  $T_w = 8^\circ\text{C}$  are given in Fig. 15. The

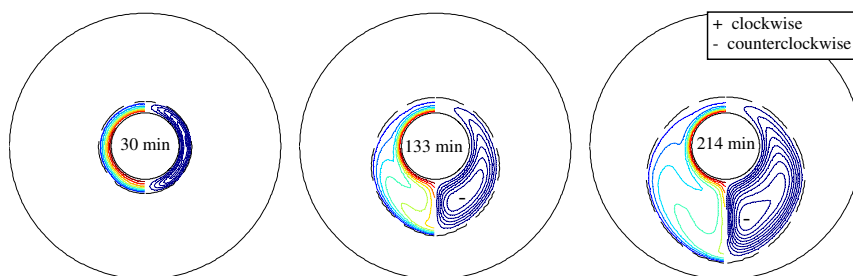


Figure 13: The temperature field (left) and the flow field (right) for  $T_w = 4^\circ\text{C}$ .

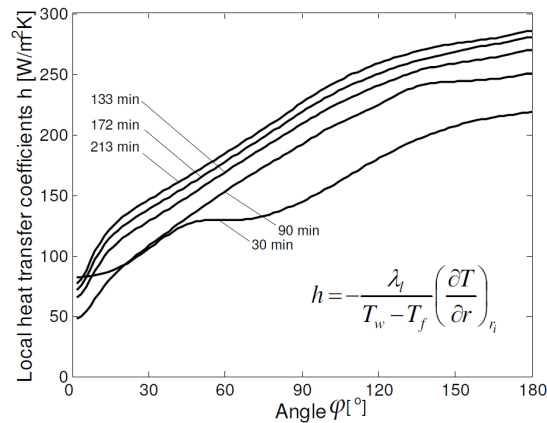


Figure 14: Local heat transfer coefficients for  $T_w = 4^\circ\text{C}$ .

ice-water interface retains the circular shape over a relatively longer period of time. As melting continues, the flow in the outer vortex, next to the ice-water interface, intensifies and occupies most of the melted region and, as a result, the movement of the interface is determined by the flow in the outer vortex and melting is more intense under the heat source.

Local heat transfer coefficients referring to the heat transfer from the inner pipe surface to the water for  $t = 67\text{min}$  (Fig. 16) have minimum values for  $\varphi \approx 100^\circ$ , i.e., on the contact of the inner and the outer vortex where temperature gradients measure a minimum. For  $\varphi < 100^\circ$ , local heat transfer coefficients are relatively lower since there is a clockwise circulation in the inner vortex down the isotherm  $T = 4^\circ\text{C}$  and then along the surface of cylinder  $T_w = 8^\circ\text{C}$ . For  $\varphi > 100^\circ$ , local heat transfer coefficients are relatively higher since there is a counterclockwise circulation of water in the outer vortex, along the surface of ice  $T_f = 0^\circ\text{C}$  and then down the warm surface of cylinder  $T_w = 8^\circ\text{C}$ .

For  $T_w = 13.6^\circ\text{C}$  (Fig. 17), at the very beginning of process, the melted region becomes pear-shaped and is facing upwards. Melting is more intense above the heat source, and retarded over quite a long period under the cylinder where the heat transfer is conduction dominated.

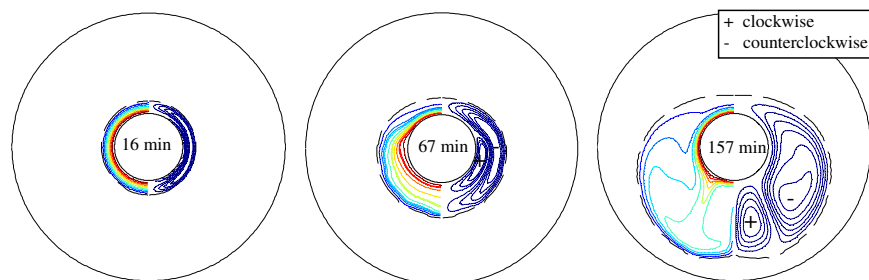


Figure 15: The temperature field (left) and the flow field (right) for  $T_w = 8^\circ\text{C}$ .

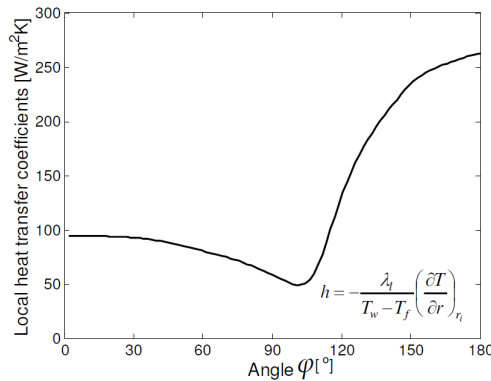


Figure 16: Local heat transfer coefficients for  $T_w = 8^\circ\text{C}$ .

The average values of heat transfer coefficients referring to the heat transfer from the inner pipe surface to the water for  $T_w = 4, 8$  and  $12^\circ\text{C}$  are presented in Fig. 18. Initial high values are characteristic for transient conduction dominated heat transfer. After 16,000 seconds for  $T_w = 4^\circ\text{C}$  and 12,000 seconds for  $T_w = 8^\circ\text{C}$ , the water comes into contact with the outer insulated pipe of the annulus and therefore, there is a drop in average heat transfer coefficients. The variation of molten volume ratio  $V/V_o$  ( $V$ -volume of molten region,  $V_o$  volume of heat source) with time is given on Fig. 19, together with the experimental data of White et al. [5] for  $T_w = 4, 8$  and  $10^\circ\text{C}$ .

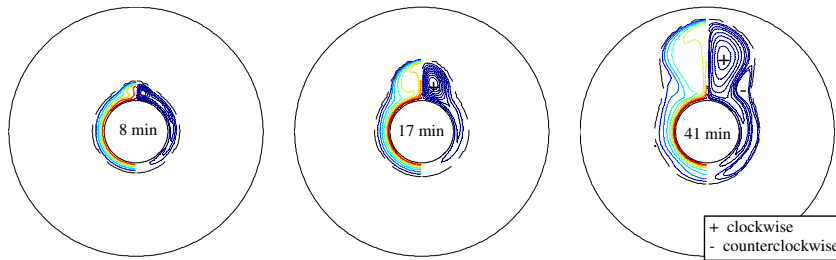


Figure 17: The temperature field (left) and the flow field (right) for  $T_w = 13.6^\circ\text{C}$ .

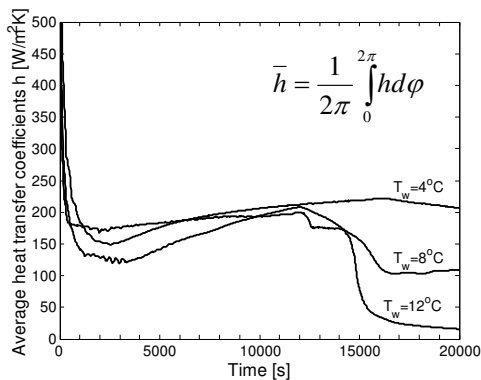


Figure 18: Average heat transfer coefficients as a function of time for different wall temperatures.

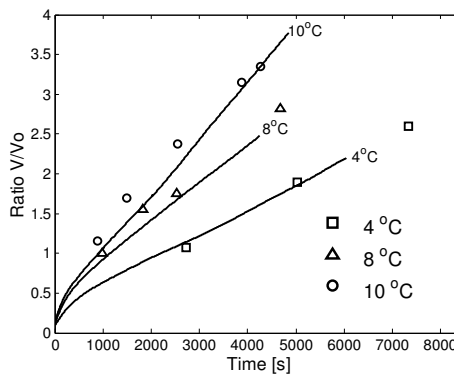


Figure 19: Variation of molten volume with time.

## 4 Conclusions

Isothermal phase change phenomena, such as water freezing and ice melting, are successfully simulated using a single domain enthalpy-based model. Performed calculations exhibit qualitatively good agreement with the available experimental [15] and other numerical results [16] for the same geometry. The obtained numerical results indicate that with such boundary conditions, natural convection has negligible influence in the case of freezing. The convection in the liquid has no significant influence on the rate of the freezing process and on the shape of the solid-liquid interface. The time needed for the complete solidification of water in the annulus strongly depends on the temperature of the heat sink and that is the inner pipe wall. Heat conduction resistance is increased as the thickness of the ice layer increases, and, therefore, the rate of solidification is slower.

On the other side, in the case of melting, the temperature of the inner cylinder wall strongly affects the flow in the liquid and the shape of solid-liquid interface. For the inner pipe temperatures under or equal to  $4^{\circ}\text{C}$ , the water with the highest density is located next to the inner wall and the flow is directed to the bottom of annulus causing a pear-shaped melted region to appear on the bottom of annulus and the highest heat transfer coefficient on the top of annulus. With inner wall temperature  $T_w$  above  $4^{\circ}\text{C}$ , the isotherm with the highest water density moves through the liquid region, and separates two distinct cells with opposite flow directions. Higher wall temperatures move maximum density isotherm closer to the phase-change interface and causes the supremacy of the clockwise flow in the liquid, forming a pear-shape on the top side of annulus.

To the authors' knowledge, fixed grid enthalpy-based method has not been previously used for the analysis of ice-water isothermal phase change in the geometry of horizontal cylindrical annulus. It would be valuable to have several benchmark results for this problem, obtained by using different numerical approaches as a reference for qualitative, as well as quantitative comparison.

## Nomenclature

$C$	$[\text{kg}/\text{m}^3\text{s}]$	constant in Darcy law
$g$	$[\text{m}^2/\text{s}]$	acceleration of gravity
$g_s$		volumetric fraction of liquid
$h$	$[\text{J}/\text{kg}]$	sensible enthalpy
$H$	$[\text{J}/\text{kg}]$	total enthalpy
$\Delta H$	$[\text{J}/\text{kg}]$	latent heat content
$k$		iteration step
$L$	$[\text{J}/\text{kg}]$	latent heat of phase change
$p$	$[\text{Pa}]$	pressure
$q$		small constant to avoid dividing by zero

$r$	[m]	radial coordinate
$r_i$	[m]	inner pipe radius
$r_o$	[m]	outer pipe radius
$r_s$	[m]	radius of ice surface
$S_h$	[W/m <sup>3</sup> ]	source term in energy equation
$S_r, S_\phi$	[J/m <sup>3</sup> ]	source terms in momentum equations
$T$	[°C]	temperature
$T_f$	[°C]	temperature of phase change
$T_i$	[°C]	initial temperature
$T_w$	[°C]	temperature of the inner pipe wall
$t$	[s]	Time
$\vec{V}$	[m/s]	velocity vector
$v_r, v_\phi$	[m/s]	component of velocity vector in polar coordinates

#### Greek symbols

$\beta$	[K <sup>-1</sup> ]	coefficient of thermal expansion
$\lambda$	[W/mK]	thermal conductivity
$\mu$	[Pas]	dynamic viscosity
$\rho$	[kg/m <sup>3</sup> ]	density
$\phi$	[°]	angular coordinate

#### Subscripts

$l$		liquid
$r$	[m]	radial
$ref$		Reference
$s$		solid
$\phi$	[°]	angular

## References

- [1] K. C. CHENG, AND N. SEKI, *Freezing and Melting Heat Transfer in Engineering: Selected Topics on Ice-Water Systems and Welding and Casting Processes*, Hemisphere, New York, 1991.
- [2] J. DANTZIG, AND M. RAPPAZ, *Solidification*, EPFL-Press, 2009.
- [3] R. VISKANTA, *Natural convection in melting and solidification*, in: S. Kakaç et al. (Eds.), *Natural Convection: Fundamentals and Applications*, Hemisphere, Washington DC, 1985, pp. 845–877.
- [4] J. STEFAN, *Über die Theorie der Eisbildung, insbesondere über die Eisbildung in Polarmeere*, *Annalen der Physik und Chemie*, 42 (1891), pp. 269–286.
- [5] J. CRANK, *Free and Moving Boundary Problems*, Clarendon Press, Oxford, 1984.
- [6] V. R. VOLLER, *An overview of numerical methods for solving phase change problems*, in *Advances in Numerical Heat Transfer* (Eds. W. J. Minkowycz and E. M. Sparrow), Taylor & Francis, New York, 1997, pp. 341–380.

- [7] M. R. ALBERT, AND K. O'NEILL, *Moving boundary-moving mesh analysis of phase change using finite elements with transfinite mappings*, Int. J. Numer. Methods. Eng., 16 (1990), pp. 465–506.
- [8] M. R. LYNCH, *Unified approach to simulation on deforming elements with application to phase change problems*, J. Comput. Phys., 47 (1986), pp. 591–607.
- [9] V. R. VOLLER, AND C. R. SWAMINATHAN, *Fixed grid techniques for phase change problems: a review*, Inter. J. Numer. Methods. Eng., 30 (1990), pp. 875–898.
- [10] V. R. VOLLER, AND C. PRAKASH, *A fixed grid numerical methodology for convection diffusion mushy region phase change problems*, Int. J. Heat. Mass. Trans., 30/8 (1987), pp. 1709–1719.
- [11] İ. DİNÇER, AND M. A. ROSEN, *Thermal Energy Storage: Systems and Applications*, John Wiley & Sons, New York, 2001.
- [12] B. ZALBA, J. M. MARIN, L. F. CABEZA, AND H. MEHLING, *Review on thermal energy storage with phase change: materials, heat transfer analysis and applications*, Appl. Thermal. Eng., 23 (2003), pp. 251–283.
- [13] A. SAITO, *Recent advances in research on cold thermal energy storage*, J. Refr., 25 (2002), pp. 177–189.
- [14] L. S. YAO, AND J. PRUSA, *Melting and freezing*, Adv. Heat. Trans., 19 (1989), pp. 1–95.
- [15] D. WHITE, R. VISKANTA, AND W. LEIDENFROST, *Heat transfer during melting of ice around a horizontal, isothermal cylinder*, Exp. Fluids., 4 (1986), pp. 171–179.
- [16] C. J. HO, AND S. CHEN, *Numerical simulation of melting of ice around a horizontal cylinder*, Int. J. Heat. Mass. Trans., 29/9 (1986), pp. 1359–1369.
- [17] W. D BENNON, AND F. P. INCROPERA, *A continuum model for momentum, heat and species transport in binary solid-liquid phase change systems-I, model formulation*, Int. J. Heat. Mass. Trans., 10 (1986), pp. 2161–2170.
- [18] S. V PATANKAR, *Numerical Heat Transfer and Fluid Flow*, Hemisphere, New York, 1980.
- [19] T. SAITOH, AND K. HIROSE, *Numerical method for the two-dimensional freezing problem around a horizontal cylinder encompassing a density inversion point*, B. JSME., 187/20 (1981), pp. 147–152.